

FIG. 2. Decay of oscillations for a "square" distribution of field inhomogeneities.

$=\gamma^2\langle h^2\rangle_{Av}t^2$  but by  $\langle\varphi^2\rangle_{Av}=\gamma^2\langle h^2\rangle_{Av}t$  according to the well-known solution of the Gaussian random walk problem.

Field inhomogeneities produce an extra phase shift  $\varphi(t)=\gamma\delta t$ . In order to obtain the whole signal we have to integrate over all values of  $\delta$ . An extra decay of the oscillations follows, described by the Fourier transform  $F(t)$  of the distribution function  $\psi(\delta)$  of  $\delta$  over the sample. The envelope amplitude of the signal is the product,

$$A=\exp(-t/T_2)F(t).$$

Discrimination between the two effects is possible for special forms of  $F(t)$ .

There are two cases of particular interest:

I. We assume that  $F(t)$  is a uniformly decreasing function of time. For example, this is the case when  $\psi(\delta)$  is a bell-shaped function or a damped oscillation function. Then the signal aspect is that given in Fig. 1 and it is not possible to obtain from its decay curve a measure of  $T_2$  if  $F(t)$  is an unknown function. But if  $F(t)$  is a periodic function of time, it is possible to draw information about  $F(t)$  from the position of successive zeros. This is the case when  $\psi(\delta)$  is a pulse-like function, and the study of signal decay is a convenient way to measure  $T_2$ .

For instance, when  $\psi(\delta)=1/\Delta$  if  $|\delta|\leq\Delta$  and  $\psi(\delta)=0$  for  $|\delta|>\Delta$ , then

$$F(t)=\sin\Delta t/\Delta t,$$

and the signal is represented on Fig. 2. Measurement of the first zero time  $t$  gives the value of  $\Delta$  from  $\Delta t=\pi$ . Then the amplitude ratio at successive maxima, which is only determined by  $T_2$  and  $\Delta$ , provides a measure of  $T_2$ . We obtain

$$T_2=\frac{3\pi}{2}/\Delta\log\left(\frac{2e_1}{3e_2}\right).$$

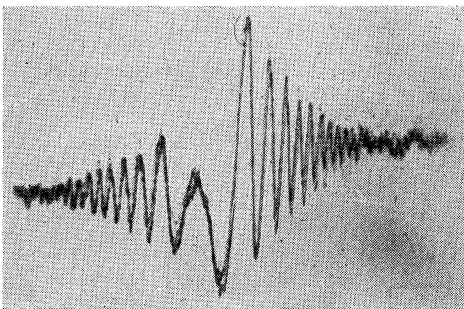


FIG. 3. Preresonance signal for  $T_2>T_0$ .

II. It is clear that  $F(t)=\int_0^\infty\psi(\delta)\cos\gamma\delta t d\delta$  is an even function. On the other hand,  $F(t)$  must be a periodic function of time  $t$  with a period  $T_0$  (half-period of the modulating field). From these two properties it follows that

$$F(T_0-t)=F(t).$$

In the presence of very large inhomogeneities,  $F(t)$  drops rapidly to zero in a time  $\tau\ll T_2$  and increases again at time before the next resonance according to the even properties of  $F(t)$ .

Then:

(A) If  $T_2<T_0$ , the factor  $\exp[(T_0-\tau)/T_2]$  is practically zero and there is no observable signal before resonance (Fig. 1 and Fig. 2).

(B) But if  $T_2>T_0$ , then  $\exp[(T_0-\tau)/T_2]$  is an important factor and we can observe a signal before resonance, as seen in Fig. 3. The ratio of the signal amplitudes,  $e_1$  after resonance and  $e_2$  before resonance, is

$$\frac{e_1}{e_2}=\exp\left(\frac{T_0-t}{T_2}\right)\frac{F(T_0-t)}{\exp(t/T_2)F(t)},$$

and if  $t\rightarrow 0$  (observations of signal near resonance) we get

$$T_2=T_0\log(e_2/e_1).$$

A limit to this method is set by random magnetic field fluctuations produced by the magnet power supplies. These fluctuations produce phase shifts strictly identical to those produced by molecular fields. These phase shifts introduce extra decays which are not generally even functions of time and are not eliminated like  $\delta$  by the previous method. In our apparatus this limit occurs for  $T_2>0.1$  sec.

Use of a permanent magnet would probably allow the measurement of times  $T_2>0.1$  sec, but it is probable that the inhomogeneous magnetic field will set a new limit here.

- <sup>1</sup> Bradford, Clay, and Strick, *Phys. Rev.* **84**, 157 (1951); Strick, Bradford, Clay, and Craft, *Phys. Rev.* **84**, 363 (1951).  
<sup>2</sup> R. Gabillard, *Compt. rend.* **232**, 324 (1951).  
<sup>3</sup> R. Gabillard, *Compt. rend.* **232**, 1477, 1551 (1951).  
<sup>4</sup> J. S. Gooden, *Nature* **165**, 1015 (1950).

## High Energy Nucleon-Deuteron Scattering\*

P. B. DAITCH AND J. B. FRENCH  
*University of Rochester, Rochester, New York*  
 (Received December 31, 1951)

WE consider the relationship between high energy nucleon-deuteron scattering and elementary nucleon-nucleon scattering. We find that one may, for the case of central potentials of arbitrary exchange character, write the nucleon-deuteron differential cross section in terms of the elementary cross sections. Except for a term which is important only in the backward direction, the reduction is simple and enables one to examine easily the arbitrariness caused by the fact that nucleon-nucleon scattering measurements do not give singlet and triplet cross sections separately nor the phases.

The quartet and doublet Born approximation matrix elements are given by<sup>1</sup>

$$M_q=(3\pi/m)(U_q+L_q+D_q), \quad M_d=(3\pi/m)(U_d+L_d+D_d), \quad (1)$$

$$\text{and} \quad d\sigma/d\omega=\frac{2}{3}|U_q+L_q+D_q|^2+\frac{1}{3}|U_d+L_d+D_d|^2, \quad (2)$$

where

$$U=(m/3\pi)\iint\chi^*\varphi^*(S)e^{-ik\cdot X}VU(1,3)e^{ik_0\cdot X}\varphi(S)\chi dXdS,$$

$$L=(m/3\pi)\iint\chi^*\varphi^*(S)e^{-ik\cdot X}(1-T_{23})V^L(2,3)$$

$$\times e^{ik_0\cdot X}\varphi(S)\chi dXdS, \quad (3)$$

$$D=(m/3\pi)\iint\chi^*\varphi^*(S)e^{-ik\cdot X}T_{23}VU(1,3)$$

$$\times e^{ik_0\cdot X}\varphi(S)\chi dXdS.$$

Here the index 3 refers to the incident nucleon; 1, 2 are particles in the deuteron with 2 and 3 referring to like nucleons;  $\chi$  is a 3-particle quartet or doublet spin wave function;  $\varphi(S)$  is the deuteron space wave function with  $\mathbf{S}=\mathbf{r}_1-\mathbf{r}_2$ ;  $\mathbf{X}$  is the coordinate of the incident nucleon with respect to the deuteron center of mass;  $\mathbf{k}_0, \mathbf{k}$  are the nucleon incident and final momenta ( $k^2=k_0^2=8mE_0/9$ , where  $E_0$  is the incident lab energy);  $T$  is the total exchange operator;  $V^U$  and  $V^L$  are unlike and like particle potentials; and  $m$ =nucleon mass.

In  $U$  we transform variables by  $\mathbf{X}=-\frac{3}{4}\boldsymbol{\rho}-\frac{1}{2}\boldsymbol{\zeta}$ ,  $\mathbf{S}=\frac{1}{2}\boldsymbol{\rho}-\boldsymbol{\zeta}$ . Then

$$U=(m/3\pi)\int\int\chi^*\varphi^*(|\boldsymbol{\zeta}-\frac{1}{2}\boldsymbol{\rho}|)\exp[i\mathbf{k}\cdot(\frac{3}{4}\boldsymbol{\rho}+\frac{1}{2}\boldsymbol{\zeta})]V^U(\rho)\times\exp[-i\mathbf{k}_0\cdot(\frac{3}{4}\boldsymbol{\rho}+\frac{1}{2}\boldsymbol{\zeta})]\varphi(|\boldsymbol{\zeta}-\frac{1}{2}\boldsymbol{\rho}|)\chi d\boldsymbol{\rho}d\boldsymbol{\zeta}. \quad (4)$$

For the nonspace exchange part of  $V^U$ , a translation of  $\boldsymbol{\zeta}$  leads to a separated integral. For the space exchange part we approximate  $\chi^*(|\boldsymbol{\zeta}+\frac{1}{2}\boldsymbol{\rho}|)\chi(|\boldsymbol{\zeta}-\frac{1}{2}\boldsymbol{\rho}|)$  by  $|\chi(\boldsymbol{\zeta})|^2$  and once again get separation. The result is

$$U\approx(m/3\pi)S^{\frac{1}{2}}(\Delta\mathbf{k})\int\chi^*\exp[-i(\frac{3}{8}\mathbf{k}-\frac{1}{8}\mathbf{k}_0)\cdot\boldsymbol{\rho}]V^U(\rho)\times\exp[i(\frac{3}{8}\mathbf{k}_0-\frac{1}{8}\mathbf{k})\cdot\boldsymbol{\rho}]\chi d\boldsymbol{\rho}, \quad (5)$$

where  $S(\Delta\mathbf{k})$  is the deuteron form factor<sup>1</sup> and  $\mathbf{k}=\mathbf{k}-\mathbf{k}_0$ . Since  $V^U$  is independent of particle 2, we eliminate the spin functions of 2 by expanding  $\chi$  in terms of the singlet and triplet spin states for particles 1, 3. The integral then appears as a matrix element for  $n-p$  scattering. Specifically we have

$$U_q=(4/3)S^{\frac{1}{2}}(\Delta\mathbf{k})^{(3)}f(\epsilon, \psi), \quad (6)$$

$$U_d=\frac{1}{3}S^{\frac{1}{2}}(\Delta\mathbf{k})\{(3)f(\epsilon, \psi)+3^{(1)}f(\epsilon, \psi)\},$$

where  $^{(3)}f(\epsilon, \psi)$ ,  $^{(1)}f(\epsilon, \psi)$  are the triplet and singlet  $n-p$  scattering amplitudes ( $d\sigma^{n,p}=\frac{3}{4}|^{(3)}f|^2+\frac{1}{4}|^{(1)}f|^2$ ) for a lab energy  $\epsilon$  and cm scattering angle  $\psi$ . The quantities  $\epsilon$  and  $\psi$  are given in terms of  $E_0$  and  $\theta$  (the nucleon deuteron c.m. scattering angle) by

$$\epsilon=E_0(25-7\cos\theta)/18, \quad \cos\psi=(-7+25\cos\theta)/(25-7\cos\theta). \quad (7)$$

An exactly similar treatment gives  $L$  in terms of like particle scattering. Except at backward angles,  $U$  and  $L$  dominate the scattering and therefore nucleon deuteron scattering is correlated in energy and angle by (7). The energy ratio increases with angle from unity at  $0^\circ$  to 1.8 at  $180^\circ$ .  $\psi$  differs little from  $\theta$ .

$D$ , however, involves the three particles in an essential fashion and cannot be reduced in the same way. It may be simply evaluated if one uses the Serber  $n-p$  potential and leads then to  $D_q=-2D_d=-(m/3\pi)I_3$ , where  $I_3$  is given by Chew.<sup>1</sup> On the other hand, by using the deuteron Fourier transform

$$\bar{\varphi}(\mathbf{p})=(2\pi)^{-3}\int\varphi(\mathbf{S})e^{i\mathbf{p}\cdot\mathbf{S}}d\mathbf{S},$$

we may write  $D$  in terms of the  $n-p$  triplet scattering as

$$D_q=-2D_d=-(4/3)\varphi(|\mathbf{k}+\frac{1}{2}\mathbf{k}_0|)\int^{(3)}f(\epsilon', \psi')\bar{\varphi}^*(\mathbf{p})d\mathbf{p}, \quad (8)$$

where  $^{(3)}f(\epsilon', \psi')$  is as defined previously the triplet  $n-p$  scattering amplitude for  $\mathbf{K}_0$  going to  $\mathbf{K}_1$ , where  $\epsilon'$  and  $\psi'$  are determined by the equations

$$2K^2=2K_0^2=p^2+(\frac{1}{2}\mathbf{k}+\mathbf{k}_0)^2, \quad \mathbf{K}\cdot\mathbf{K}_0=\mathbf{p}\cdot(\frac{1}{2}\mathbf{k}+\mathbf{k}_0). \quad (9)$$

The nucleon-deuteron cross section now appears in the form

$$d\sigma/d\omega(E_0, \theta)=\frac{3}{4}|(4/3)S^{\frac{1}{2}}(\Delta\mathbf{k})^{(3)}f+^{(3)}g+D_q|^2+\frac{1}{3}|S^{\frac{1}{2}}(\Delta\mathbf{k})^{(3)}f+3^{(1)}f+^{(3)}g+3^{(1)}g+D_d|^2, \quad (10)$$

where the  $f$ 's and  $g$ 's are unlike and like particle scattering amplitudes for  $\epsilon, \psi$  as given by (7).

We note that since the  $n-p$  and  $p-p$  measurements do not determine the singlet and triplet amplitudes separately nor the relative phases, the scattering measurements allow a great deal of arbitrariness in calculating nucleon-deuteron scattering. For example, with 240-Mev protons at  $20^\circ$  one can easily vary the calculated  $p-d$  cross section by a factor 20 by choosing various decompositions of the nucleon-nucleon cross sections. It seems

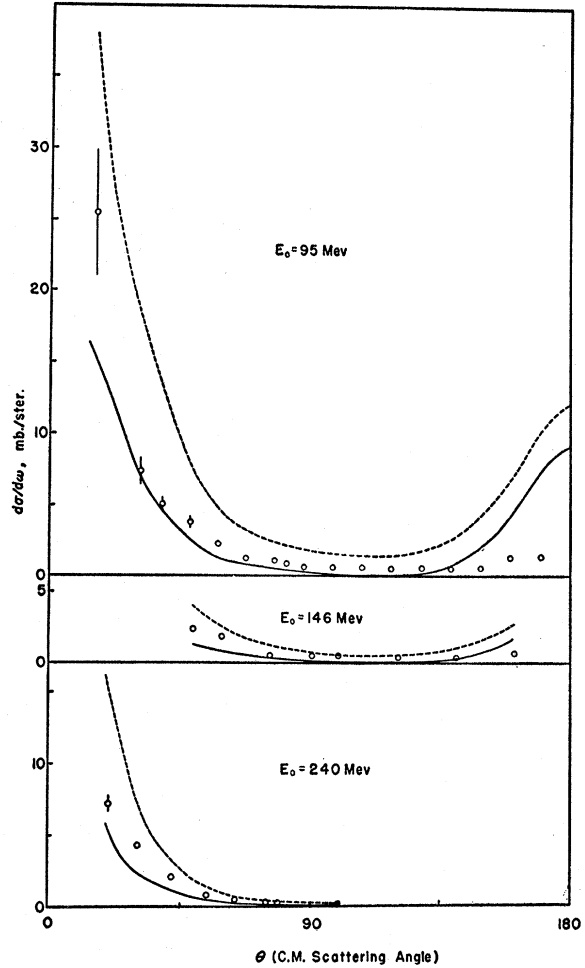


FIG. 1. Comparison of theoretical and experimental proton-deuteron elastic scattering cross section. Dashed and solid curves are: for  $p-p$  and  $n-p$  amplitudes interfering constructively ( $^{(1)}g=+1$ ) and destructively ( $^{(1)}g=-1$ ), respectively. Sources of experimental data are listed in reference 3.

reasonable, however, to determine the  $f$ 's on the basis of the Serber  $n-p$  interaction. Then we have that the signs are the same and

$$|^{(1)}f|^2=\eta^2|^{(3)}f|^2=[4\eta^2/(3+\eta^2)]d\sigma^{n,p}/d\omega, \quad (\eta=0.686). \quad (11)$$

Within the framework of central forces the only simple choice which can lead to an angular and energy independent  $p-p$  cross section is

$$^{(3)}g=0, \quad |^{(1)}g|^2=4d\sigma^{n,p}/d\omega, \quad (12)$$

with arbitrary phase of  $^{(1)}g$ .

With these determinations of the amplitudes and with relative phase of  $^{(1)}g$  as  $\pm 1$ , we plot in Fig. 1 the calculated  $p-d$  cross sections for proton energies of 95, 146, and 240 Mev. We have taken the  $p-p$  cross section to be 5 mb/sterad and have used an empirical formula for the  $n-p$  differential cross section.  $D$  was evaluated by numerically integrating (8); this gives a result little different from that given by Chew's  $I_3$ . Shown also in the figure are the available data.<sup>3</sup> The two calculated curves enclose the data except in the backward direction. The source of disagreement here is not clear. The backward scattering is a function mainly of low energy  $n-p$  scattering and low momentum Fourier components of the deuteron. For example, at 95 Mev the main contribution is from  $\epsilon$  between 20 and 150 Mev and  $p$  less than

three times its average value in the deuteron. It seems possible that the backward peak would be reduced by the inclusion of tensor forces.<sup>4</sup>

\* Assisted in part by the AEC.

<sup>1</sup> G. F. Chew, Phys. Rev. **74**, 809 (1948); R. L. Gluckstern and H. A. Bethe, Phys. Rev. **81**, 761 (1951).

<sup>2</sup> This approximation was checked by calculating the exact and approximate expressions using a Yukawa well and various energies and angles in the range of interest. At 90 Mev the agreement was everywhere within 10 percent; for large angles with higher energies the agreement is rather worse but since the exchange parts of  $U$  and  $L$  are dominant only for intermediate angles the approximation is satisfactory. We wish to thank Mr. T. A. Auerbach for making available to us his numerical evaluations for the exact integrals.

<sup>3</sup> M. O. Stern, University of California Radiation Laboratory Report No. 1440 (1951) (95-Mev data); Cassels, Stafford, and Pickavance, Nature **168**, 556 (1951) (146-Mev data); R. D. Schamberger, Phys. Rev. **83**, 1276 (1951) (240-Mev data).

<sup>4</sup> Horie, Tamura, and Yoshida, Prog. Theoret. Phys. **6**, 623 (1951).

### Some Polystyrene Solid Solutions as Scintillation Counters\*

THOMAS CARLSON AND W. S. KOSKI  
Department of Chemistry, Johns Hopkins University,  
Baltimore, Maryland

(Received December 26, 1951)

THE scintillation efficiency and the spectral emission of a number of polystyrene solid solutions have been investigated. The method of preparing the solid solutions and the experimental procedure used in obtaining the data is similar to what has been reported previously.<sup>1</sup> A 5819 photomultiplier tube was used for the counting experiments. Co<sup>60</sup> was used as a  $\gamma$ -ray source. A commercial x-ray machine was used as a source for the emission-spectra studies. The solid solutions compared were plastic disks containing 2 percent by weight of the phosphor in styrene, which were then polymerized by a 50-50 benzoyl peroxide-tricresyl phosphate catalyst. The results are summarized in Fig. 1 which gives the relative counting rates as a function of discriminator bias and in Table I where the peaks of the emission bands are recorded. It is interesting to compare these results with

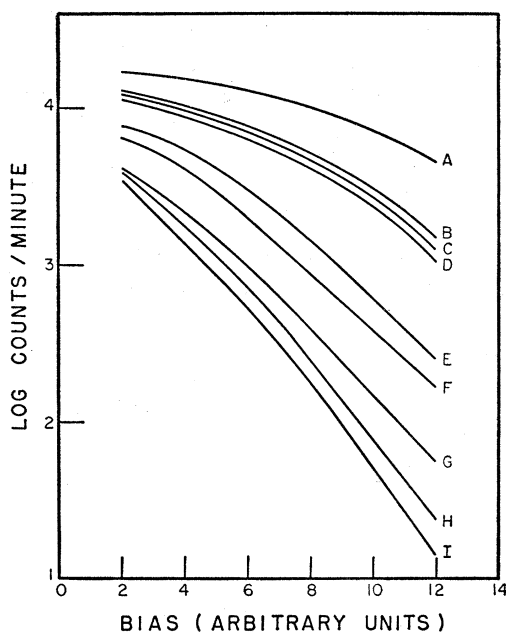


FIG. 1. Discriminator curves for some phosphor-plastic combinations: A—terphenyl; B—diphenylbutadiene; C—anthracene; D—stilbene; E—diphenylacetylene; F—biphenyl; G—diphenylacetylene; H—diphenylethane; I—polystyrene (plain).

TABLE I. Wavelengths of emission bands of various 2 percent phosphor-plastic systems excited by x-rays.

Material	Wavelength (Å)
stilbene	3760, 3600
diphenylbutadiene	4040
diphenylhexatriene	4200
diphenylacetylene	3720
diphenylidiacetylene	4610
anthracene	4475, 4235
diphenylethane	~3200
terphenyl	3620, 3480

those obtained with the single crystals of the corresponding phosphors.<sup>2</sup> It will be noted that the relative order is not always the same. A notable exception is diphenylacetylene. In the crystalline state this material compares favorably with stilbene whereas in the solid solution its performance is much poorer. Since the emission bands of the solid solution and of the crystal are located in approximately the same spectral region, a poorer counting rate cannot be ascribed to a shifting away from the region of more favorable spectral response of the 5819 photomultiplier tube.

Polystyrene-diphenylhexatriene solid solutions gave poor performances as counters. The large spectral shift toward the blue (1000Å), plus the fact that there was a considerable amount of difficulty in realizing the polymerization of the solution, indicated that there probably was a chemical reaction between phosphor and catalyst or styrene with an interruption to the conjugation of the polyene chain. The corresponding system with diphenyloctatetraene failed to polymerize satisfactorily even after prolonged heating so it is not included in these results.

We wish to acknowledge our indebtedness to Professor J. D. H. Donnay and Professor R. Maddin for the use of their x-ray machines.

\* This work was performed under the auspices of the AEC.

<sup>1</sup> W. S. Koski, Phys. Rev. **82**, 230 (1951).

<sup>2</sup> W. S. Koski and C. O. Thomas, J. Chem. Phys. **19**, 1286 (1951).

### Absence of Secondary Maxima in the Transition Curve for Electronic Showers

R. MAZE  
Laboratoire École Normale Supérieure, Paris, France  
(Received November 13, 1951)

IN a recent letter Tsai-Chü<sup>1</sup> tentatively explained the existence of a secondary maximum of the Rossi curve obtained by a counter arrangement very similar to that of Bothe and Thurin.<sup>2</sup>

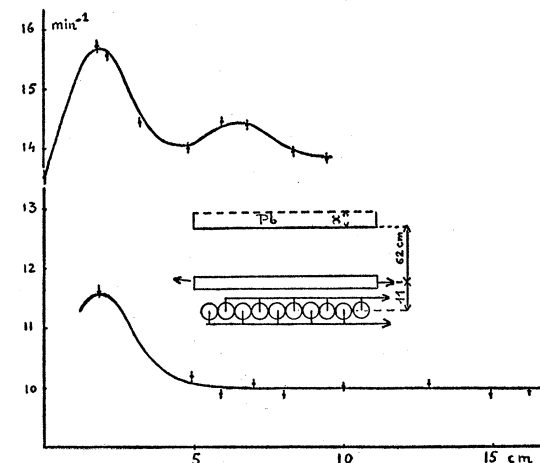


FIG. 1. Rossi curves for lead.